Error Probability Performance Prediction for Multichannel Reception of Linearly Modulated Coherent Systems on Fading Channels

Thomas L. Staley, Jianxia Luo, *Member, IEEE*, Walter H. Ku, and James R. Zeidler, *Fellow, IEEE*

***Abstract*—This paper provides a framework for the analysis of error rate performance of maximal ratio combining multichannel reception of coherent linearly modulated systems over frequency-selective fading channels. Expressions for the error probability are developed, and the special cases for which closed-form or acceptable efficient numerical solutions are possible are delineated. A new efficient and accurate recursive method for the Ricean fading main resolved path case is presented for coherent quadrature amplitude modulation constellations. The effect of automatic gain control error on analysis of modulation schemes is demonstrated. Finally, numerical examples based on the maritime high-data-rate channel model are provided to demonstrate the usefulness of the framework.**

***Index Terms*—Error probability performance, frequency-selective fading channels, quadrature amplitude modulation, Ricean channels.**

I. Introduction

THE need for spectral efficiency for high-data-rate (HDR) wireless communications systems has led to renewed interest in coherent multichannel reception of linearly modulated signals, such as *m*-ary phase-shift keying (M-PSK) and *m*-ary quadrature amplitude modulation (M-QAM), which are known to be power-efficient with small M or bandwidth-efficient with large M. Ever increasing data rates will necessitate the consideration of frequency-selective fading. The presence of a line-of-sight (LOS) propagation component, such as that in microcellular systems, gives rise to the more favorable Ricean fading environment.

The work in [1] provides the error rate analysis in flat Ricean/Rayleigh fading with multiplicative distortion compensation approach. Specific results for the square M-QAM (16- and 64-QAM) modulation are obtained for the single-channel flat Rayleigh fading case in [2]. In [3], M-QAM symbol error rate expressions involving hypergeometric functions are derived for L-branch selection combining and maximal-ratio combining in additive white Gaussian noise (AWGN) and Rayleigh fading. In his pioneering work on frequency-selective fading channels, Bello [5] derives a general error probability expression for multichannel reception of binary signals. Recently, the work of [6] provided a theoretical analysis of square 16-QAM in frequency-selective Rayleigh fading, leading to many interesting findings on effects of systems design factors. However, the above results can not be readily extended to the multichannel frequency-selective Ricean case.

In [7], the authors developed an accurate and efficient recursive solution for error probability performance evaluation of multichannel M-PSK reception in frequency-selective Ricean fading channels. This letter extends the error rate anlysis in [7] to coherent linear modulation systems, and specific results for the square M-QAM constellations are derived.

Paper approved by P. Y. Kam, the Editor for Modulation and Detection for Wireless Systems of the IEEE Communications Society. Manuscript received March 12, 2001; revised November 23, 2001 and February 13, 2001. This paper was presented in part at the IEEE Military Communications Conference, McLean, VA, October 1996.

T. L. Staley is with the Communications Department, SPAWAR Systems Center, San Diego, CA 92152 USA.

J. Luo and W. H. Ku are with the Department of Electrical and Computer Engineering, University of California at San Diego, La Jolla, CA 92093 USA.

J. R. Zeidler is with the Communications Department, SPAWAR Systems Center, San Diego, CA 92152 USA, and also with the Department of Electrical and Computer Engineering, University of California at San Diego, La Jolla, CA 92093 USA (e-mail: zeidler@spawar.navy.mil).

Publisher Item Identifier 10.1109/TCOMM.2002.802555.

II. Signal and Channel Model

The signal model of interest is the general linear memoryless model represented by

$$u(t) = \sum_k I_{i_k} p_T(t - kT), \qquad i_k \in 1, 2, \ldots, M \tag{1}$$

where I_{i_k} is the complex information symbol transmitted during the kth interval, T is the symbol duration, and $p_T(t)$ is the transmitter pulse-shaping waveform such that $p(t) = p_T(t)^* p_T^*(-t)$ satisfies the Nyquist pulse criterion and is band limited to W_p and is scaled such that $\int_{-\infty}^{\infty} p(t)\, dt = 1$. The energy per symbol for the ith symbol and the average energy per bit are given by

$$E_{s,i} = \frac{1}{2} |I_i|^2 \text{ and } E_b = \frac{1}{M \log_2 M} \sum_{i=1}^{M} E_{s,i}. \tag{2}$$

Each of the multiple channels is a band-limited channel, This "resolved channel" is assumed to have resulted from an underlying slowly fading wide-sense stationary uncorrelated scattering (WSSUS) complex Gaussian channel $h_l'(\tau)$ convolved with an ideal low-pass filter $f_{\mathrm{LP}}(t)$ with bandwidth $W \geq W_p$ which represents the receiver front-end bandpass filter. The important consequences of using the resolved channel model for performance prediction was demonstrated in [7]. The resolved channels are thus given by the two-sided finite-impulse response (FIR) model

$$h_l(\tau) = \underbrace{|h_{l,0}| \exp(j\phi_{l,0})\delta(\tau)}_{h_{l,0}} + \underbrace{\sum_{\substack{n=-N_L \\ n\neq 0}}^{N_U} h_{l,n}\delta\left(\tau - \frac{nT}{c}\right)}_{\tilde{h}_l(\tau)},$$
$$l \in 1, 2, \ldots, L \text{ with } N_U, N_L \text{ s.t. } h_l(\tau) \approx 0 \text{ for } \tau < \frac{-N_L T}{c} \text{ and } \tau > \frac{N_U T}{c}\ \forall l. \tag{3}$$

where $h_{l,n} = h_l(nT/c)$ are the resolved path coefficients and c is chosen to meet or exceed the Nyquist rate. In (3), $h_{l,0}$ repre-

0090-6778/02$17.00 © 2002 IEEE

sents the main resolved path, usually the direct path, and $\bar{h}_l(\tau)$ represents the resolved multipath. The complex Gaussian $h_{l,n}$ can be zero or nonzero mean, corresponding to Rayleigh or Ricean fading, respectively, on the nth path. Each of the multiple channels is assumed to fade independently and with identical distributions. Each channel is also corrupted by AWGN with a spectral density of N_0. Without loss of generality and restricting attention to the $k = 0$ signaling interval, the decision statistic for the general linear modulation can be written as [7]

$$Z \equiv Z_0 = \sum_{l=1}^{L} \left(|h_{l,0}|^2 \vec{I}^H \vec{p} + \vec{I}^H G \vec{\bar{h}}_l h_{l,0}^* + n_l h_{l,0}^* \right) \quad (4)$$

where the definitions of $\vec{I}$, G, $\vec{\bar{h}}_l$, and n_l are the same as those in [7]. The decision statistics (4) are decomposed into main resolved path, resolved multipath, and noise components, respectively. Conditioned on the $h_{l,0}$'s, the decision statistic (4) is a complex Gaussian random variable with the mean [7]

$$\hat{m} = \sum_{l=1}^{L} \left[|h_{l,0}|^2 \left(\vec{I}^H \vec{p} + \vec{I}^H \frac{G\vec{\phi}}{\sigma_0^2} \right) + \vec{I}^H G \left(\vec{\bar{m}} - \frac{m_0}{\sigma_0^2} \vec{\phi} \right) h_{l,0}^* \right] \quad (5)$$

and covariance

$$\hat{\sigma}^2 \equiv \sum_{l=1}^{L} |h_{l,0}|^2 \left(N_0 + \vec{I}^H \phi_x \vec{I} \right)$$

where

$$\phi_x = G \left(\phi_{\bar{h}} - \frac{1}{\sigma_0^2} \vec{\phi} \vec{\phi}^H \right) G^H. \quad (6)$$

III. Probability of Error Expressions for Linear Modulation

The probability of symbol and bit errors are given by

$$P_s = M^{-K_T} \sum_{\{\vec{I}\}} P_{s|\vec{I}} \text{ and } P_b = M^{-K_T} \sum_{\{\vec{I}\}} P_{b|\vec{I}} \quad (7)$$

where $K_T = \lceil N_L/c + t_{\max}/T \rceil + \lceil N_U/c + t_{\max}/T \rceil + 1$. Also, $P_{s|\vec{I}} = 1 - \Pr(Z \in R_{i_0})$ is the conditional symbol error probability, and R_{i_0} is the region in decision space that is mapped to symbol I_{i_0}. The conditional bit error probability is given by $P_{b|\vec{I}} = \sum_{i=1}^{M} \Pr(Z \in R_{I_i})(\epsilon_i)$ where ϵ_i is the number of bit errors corresponding to R_{I_i} and is dependent on the bits-to-symbols mapping.

The sums of (7) involve M^{K_T} repetitions of the conditional probability evaluation, so that it is critical that the evaluation $\Pr(Z \in R_{I_i})$ has either a closed form or an efficient numerical solution. The authors of [7] developed the recursive solution for the error probability of M-PSK reception. In this letter, we focus on M-QAM modulation. For the $M = 2$ case, the decision statistics correspond to comparing $\mathrm{Re}[Z(I_1^* - I_2^*)]$ to a zero threshold, and the probability of bit error is given by

$$P_b = 2^{-K^T} \sum_{\{\vec{I}\}}{}' \Big[\Pr\left(\mathrm{Re}[Z(I_1^* - I_2^*)] < 0 \mid \vec{I}, i_0 = 1 \right) + \Pr\left(\mathrm{Re}[Z(I_1^* - I_2^*)] > 0 \mid \vec{I}, i_0 = 2 \right) \Big] \quad (8)$$

where the primed sum excludes I_{i_0}. The desired probabilities in (8) are a special case of the expression in [8, Appendix B] with $C = I_1^* - I_2^*$.

For $M > 2$, evaluation of the conditional probabilities in (7) involves determining the probability that the decision statistic falls within a particular region of decision space, which is represented by

$$J_{Z_r}(z, i_0) \equiv \Pr\left(\mathrm{Re}[Z] < z \mid \vec{I}, I_{i_0} \right)$$
$$J_{Z_i}(z, i_0) \equiv \Pr\left(\mathrm{Im}[Z] < z \mid \vec{I}, I_{i_0} \right). \quad (9)$$

The second component of the mean term of (5) makes it difficult to obtain efficient solutions for (9), and an acceptable solution for the most general case of frequency-selective Ricean fading on all paths is not available. Fortunately, there are special cases of practical importance for which acceptable solutions are possible, and this is the focus of Sections III-A and B.

A. Ricean-Fading Main Resolved Path Case

When a specular component exists, such as in environments with a line-of-sight (LOS) component, and the main path experiences Ricean fading, there are two cases of interest.

Case I: flat Ricean fading occurs when $m_0 \neq 0$ and $\vec{I}^H \phi_x \vec{I} \approx 0$, $G\vec{\phi} \approx \vec{0}$, and $G\vec{\bar{m}} \approx \vec{0}$.

In this case, (5) and (6) simplify to

$$\hat{m} = \sum_{l=1}^{L} |h_{l,0}|^2 \vec{I}^H \vec{p} \equiv \gamma \cdot A e^{j\alpha}$$

and

$$\hat{\sigma}^2 = \sum_{l=1}^{L} |h_{l,0}|^2 N_0 \equiv \gamma \cdot \sigma^2 \quad (10)$$

where

$$\gamma \equiv \sum_{l=1}^{L} |h_{l,0}|^2, \sigma^2 \equiv N_0 \text{ and } A \exp^{j\alpha} \equiv \vec{I}^H \vec{p}. \quad (11)$$

Case II: frequency-selective fading occurs when $\vec{I}^H G \left(\vec{\bar{m}} - (m_0/\sigma_0^2)\vec{\phi} \right) \approx 0$.

Similarly, we can define the following notations with the same approximation outlined in [7]:

$$\gamma \equiv \sum_{l=1}^{L} |h_{l,0}|^2,$$
$$A \exp^{j\alpha} \equiv \vec{I}^H \vec{p} + \frac{1}{\sigma_0^2(K+1)} \vec{I}^H G\vec{\phi} + \frac{K}{m_0(K+1)} \vec{I}^H G\vec{\bar{m}}$$
$$\sigma^2 \equiv N_0 + \vec{I}^H \phi_x \vec{I} + \vec{I}^H G \left(\vec{\bar{m}} - \frac{m_0}{\sigma_0^2} \vec{\phi} \right) \times \left(\vec{\bar{m}} - \frac{m_0}{\sigma_0^2} \vec{\phi} \right)^H G^H \vec{I} \frac{1}{(K+1)}, \qquad K \equiv \frac{m_0}{2\sigma_0^2}. \quad (12)$$

Given the mean and variance of the Gaussian random variable, (9) can be directly written as

$$J_{Z_r}(z, i_0) = \int_0^\infty p(\gamma) \Phi \left(\frac{z - \gamma A \cos\alpha}{\sqrt{\gamma}\sigma} \right) d\gamma$$
$$J_{Z_i}(z, i_0) = \int_0^\infty p(\gamma) \Phi \left(\frac{z - \gamma A \sin\alpha}{\sqrt{\gamma}\sigma} \right) d\gamma \quad (13)$$

where

$$\Phi(x) \equiv \frac{1}{\sqrt{2\pi}} \int_{-\infty}^{x} \exp\left(-\frac{t^2}{2}\right) dt$$

$$p(\gamma) = \frac{1}{2\sigma_0^2}\left(\frac{\gamma}{Lm_0^2}\right)^{(L-1)/2} \times \exp\left(-\frac{Lm_0^2+\gamma}{2\sigma_0^2}\right) I_{L-1}\left(\frac{\sqrt{\gamma L}m_0}{\sigma_0^2}\right).$$

The expressions of (13) can be rewritten in the general form of

$$J_Z(b,c) \equiv \int_0^{\infty} p(\gamma)\Phi\left(\frac{b}{\sqrt{\gamma}} - c\sqrt{\gamma}\right) d\gamma. \tag{14}$$

In [10], an efficient and accurate recursive solution for (14) is developed, and we will recapitulate the key results as follows:

$$J_Z(b,c) = \frac{1}{2} + \frac{\mathrm{sgn}[b]}{2} - B_1 \sum_{k=0}^{L-1} d_k - B_1 \sum_{r=0}^{\infty} k_r d_{r+L} \tag{15}$$

with the recursions

$$\begin{aligned} k_r &= k_{r-1} - f_r \\ f_r &= \frac{LK}{r} f_{r-1} \\ d_r &= c\sigma_0(r+1) j_{r+1} + \frac{b}{2\sigma_0^2} j_r \\ j_r &= \frac{1}{2(1+c^2\sigma_0^2)}\left(\left(r-\frac{3}{2}\right) j_{r-1} + \frac{b^2}{4(r-1)\sigma_0^2} j_{r-2}\right) \end{aligned} \tag{16}$$

and initial conditions

$$\begin{aligned} f_0 &= \exp(-LK) \\ k_0 &= 1 - f_0 \\ d_r &= c\sigma_0(r+1) j_{r+1} + \frac{b}{2\sigma_0^2} j_r \\ j_1 &= \frac{1}{\sqrt{2}\sqrt{1+c^2\sigma_0^2}} \\ j_0 &= \begin{cases} \frac{\sigma_0\sqrt{2}}{|b|}, & b \neq 0 \\ 0, & b = 0 \end{cases} \end{aligned} \tag{17}$$

and the definitions

$$B_1 \equiv \frac{1}{\sqrt{2}} \exp\left(b\frac{c\sigma_0 - \mathrm{sgn}[b]\sqrt{1+c^2\sigma_0^2}}{\sigma_0}\right). \tag{18}$$

The truncation error incurred when the summation of (15) stopped at $r = R$ is given by

$$E_R \equiv B_1 \sum_{r=R+1}^{\infty} k_r d_{r+L}. \tag{19}$$

It is shown in [10] that the error magnitude can also be upper bounded and have recursive updates. The recursion of (15), (16), and (19) is continued until either one of the truncation error bounds fall within the desired absolute or relative error. The convergence of the recursive method is much faster than standard numerical integration techniques.

B. Rayleigh-Fading Main Resolved Path Case

Another special case for which an efficient solution of (9) is possible occurs when all of the resolved paths experience Rayleigh fading, i.e., $m_0 = 0$ and $\vec{m} = \vec{0}$. With the definitions of

$$\begin{aligned} \gamma &\equiv \sum_{l=1}^{L} |h_{l,0}|^2 \\ A\exp^{j\alpha} &\equiv \vec{I}^H\vec{p} + \vec{I}^H\frac{G\vec{\phi}}{\sigma_0^2} \\ \sigma^2 &\equiv N_0 + \vec{I}^H G\left(\phi_{\vec{h}} - \frac{1}{\sigma_0^2}\vec{\phi}\vec{\phi}^H\right) G^H\vec{I} \end{aligned} \tag{20}$$

$$p(\gamma) = \frac{1}{(L-1)!}\frac{\gamma^{L-1}}{(2\sigma_0^2)^L}\exp\left(-\frac{\gamma}{2\sigma_0^2}\right) \tag{21}$$

the closed-form solution for (14) is just a special case of (15) with $k_r = 0$, i.e.

$$J_Z(b,c) = \frac{1}{2} + \frac{\mathrm{sgn}[b]}{2} - B_1 \sum_{k=0}^{L-1} d_k. \tag{22}$$

IV. Probability of Bit Error for Gray-Encoded Linear Modulation

For many linear modulation schemes, the in-phase and quadrature bit streams are independently modulated. In such cases, bit error probabilities can then be easily written in terms of (13). One such example is the Gray-coded square M-QAM constellation. The signal constellation, decision boundaries, and bit mapping for 16-QAM are shown in [11, Fig. 4], where δ is the decision boundary parameter. We note that the first and third bits are the in-phase bit stream, while the second and fourth bits form the quadrature bit stream [2]. The in-phase and quadrature bit error probabilities are identical due to the circular symmetry resulting from the cases considered in Section III-A.

In order to develop a bit error expression for the in-phase bits, consider the conditional probability when the I_4 symbol is sent. If the real part of the decision statistic is between 0 and 2δ, a bit error occurs for the third bit. Similarly, if the real part is between -2δ and 0, two bit errors are made, and, if the real part is less than -2δ, one bit error is made. Consequently,

$$P_{b|\vec{I},i_0=4} = J_{Z_r}(0, i_0 = 4) + J_{Z_r}(2\delta, i_0 = 4) - J_{Z_r}(-2\delta, i_0 = 4). \tag{23}$$

The aforementioned circular symmetry results in the bit error probability conditioned on I_1, I_{13}, or I_{16} being the same as (23). By continuing in the same manner for the remaining symbols in

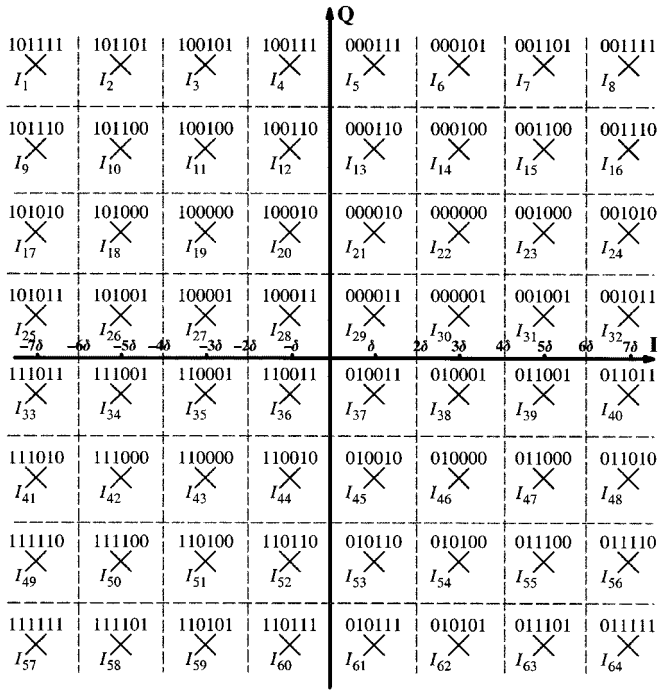

Fig. 1. 64-QAM constellation with Gray-code encoding.

the constellation, it follows that the probability of bit error can be written as

$$\begin{aligned}P_{b|\vec{I},16\text{-QAM}} =& \frac{1}{4}\left(J_{Z_r}(0,i_0=4)+J_{Z_r}(2\delta,i_0=4)\right.\\ &\left.-J_{Z_r}(-2\delta,i_0=4)\right)\\ &+\frac{1}{4}\left(1+J_{Z_r}(0,i_0=3)-J_{Z_r}(2\delta,i_0=3)\right.\\ &\left.+J_{Z_r}(-2\delta,i_0=3)\right)\\ &+\frac{1}{4}\left(1+J_{Z_r}(0,i_0=7)-J_{Z_r}(2\delta,i_0=7)\right.\\ &\left.+J_{Z_r}(-2\delta,i_0=7)\right)\\ &+\frac{1}{4}\left(J_{Z_r}(0,i_0=8)+J_{Z_r}(2\delta,i_0=8)\right.\\ &\left.-J_{Z_r}(-2\delta i_0=8)\right).\end{aligned} \tag{24}$$

When evaluating the probability of error for any modulation scheme incorporating amplitude modulation in a fading environment, the automatic gain control (AGC) of the receiver must be taken into account. The relation of the probabilities in (24) to the solution of (15)–(19) depends on the ability of the AGC to track the instantaneous value of the fading amplitude. The expression for the decision boundary parameter δ depends on the relation between the time constant of the AGC and the coherence time of the fading channel. When the time constant of the AGC is such that it fully tracks the fading, as is assumed in [1], the decision boundary parameter is given by

$$\delta=\sqrt{\frac{4}{5}E_b}\sum_{l=1}^{L}|h_{l,0}|^2=\sqrt{\frac{4}{5}E_b\gamma}. \tag{25}$$

In the worst case, as in [2], the AGC tracks the **average** value of the random fading, and

$$\delta=\sqrt{\frac{4}{5}E_b\bar{\gamma}},\qquad \text{where } \bar{\gamma}\equiv L(2\sigma_0^2+m_0^2). \tag{26}$$

This framework also allows consideration of a fixed AGC error by defining

$$\delta=\sqrt{\frac{4}{5}E_b}\left(\bar{\gamma}\epsilon_{\text{AGC}}+\gamma\left(1-\epsilon_{\text{AGC}}\right)\right) \tag{27}$$

where ϵ_{AGC} represents the AGC error. $\epsilon_{\text{AGC}}=0$ corresponds to the perfect AGC case of (25), and $\epsilon_{\text{AGC}}=1$ corresponds to the lagging AGC of (26). Using (27), the individual components of (24) can then be related to (14) as

$$\begin{aligned}J_{Z_r}(z\delta,i_0)=J_Z\left[\sqrt{\frac{4}{5}E_b}\frac{z\epsilon_{\text{AGC}}}{\sigma},\right.\\ \left.\frac{\text{Re}[A\exp^{j\alpha}]+(\epsilon_{\text{AGC}}-1)\,z\sqrt{\frac{4}{5}E_b}}{\sigma}\right].\end{aligned} \tag{28}$$

It can be easily shown from (28) that $J_{Z_r}(z,i_0)$ depends on only the real part of I_{i_0}. Consequently, (24) can be simplified to

$$\begin{aligned}P_{b|\vec{I},16\text{-QAM}} =& \frac{1}{2}\left(J_{Z_r}(0,i_0=4)+J_{Z_r}(2\delta,i_0=4)\right.\\ &\left.-J_{Z_r}(-2\delta,i_0=4)\right)\\ &+\frac{1}{2}\left(1+J_{Z_r}(0,i_0=3)-J_{Z_r}(2\delta,i_0=3)\right.\\ &\left.+J_{Z_r}(-2\delta,i_0=3)\right).\end{aligned} \tag{29}$$

Referring to Fig. 1, which depicts the constellation and bits-to-symbols mapping for 64-QAM, the bit error probability for the 64-QAM square constellation can be obtained in an analogous manner, i.e.

$$\begin{aligned}P_{b|\vec{I},64\text{-QAM}} =& \frac{1}{4}\left[1+J_{Z_r}(6\delta,i_0=5)-J_{Z_r}(4\delta,i_0=5)\right.\\ &-J_{Z_r}(2\delta,i_0=5)+J_{Z_r}(0,i_0=5)\\ &+J_{Z_r}(-2\delta,i_0=5)+J_{Z_r}(-4\delta,i_0=5)\\ &\left.-J_{Z_r}(-6\delta,i_0=5)\right]\\ &+\frac{1}{4}\left[2-J_{Z_r}(6\delta,i_0=6)-J_{Z_r}(4\delta,i_0=6)\right.\\ &+J_{Z_r}(2\delta,i_0=6)+J_{Z_r}(0,i_0=6)\\ &-J_{Z_r}(-2\delta,i_0=6)-J_{Z_r}(-4\delta,i_0=6)\\ &\left.+J_{Z_r}(-6\delta,i_0=6)\right]\\ &+\frac{1}{4}\left[1-J_{Z_r}(6\delta,i_0=7)+J_{Z_r}(4\delta,i_0=7)\right.\\ &+J_{Z_r}(2\delta,i_0=7)+J_{Z_r}(0,i_0=7)\\ &-J_{Z_r}(-2\delta,i_0=7)-J_{Z_r}(-4\delta,i_0=7)\\ &\left.+J_{Z_r}(-6\delta,i_0=7)\right]\\ &+\frac{1}{4}\left[J_{Z_r}(6\delta,i_0=8)+J_{Z_r}(4\delta,i_0=8)\right.\\ &-J_{Z_r}(2\delta,i_0=8)+J_{Z_r}(0,i_0=8)\\ &+J_{Z_r}(-2\delta,i_0=8)-J_{Z_r}(-4\delta,i_0=8)\\ &\left.-J_{Z_r}(-6\delta,i_0=8)\right].\end{aligned} \tag{30}$$

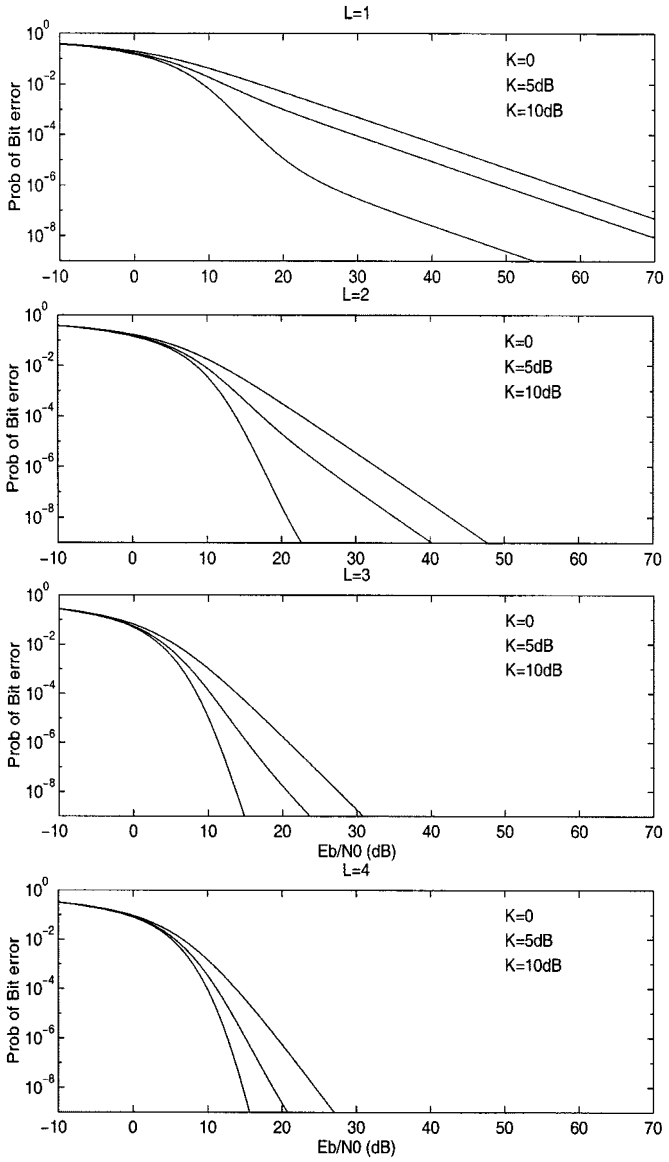

Fig. 2. P_b for 16-QAM with a varying main path K-factor in flat Ricean fading.

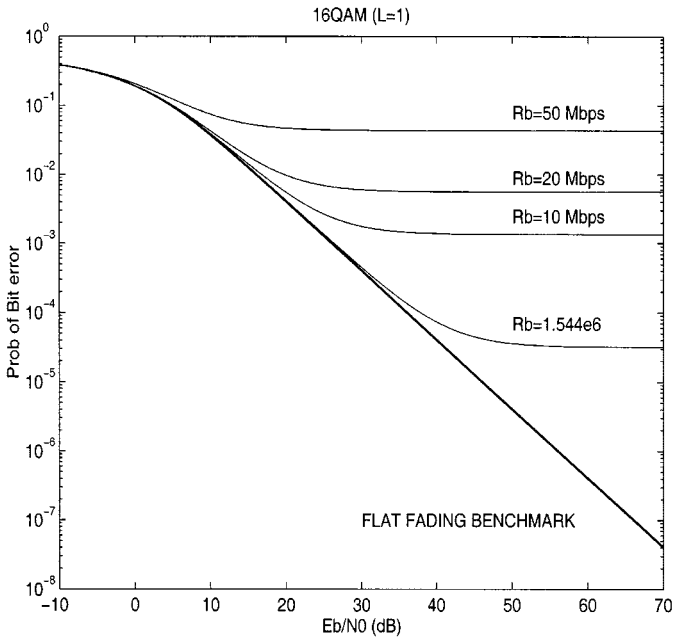

Fig. 3. P_b for the 16-QAM frequency-selective Ricean fading case.

V. Numerical Examples

This section presents a few examples to demonstrate the application of the results to 16-QAM and to consider effects important to modulation schemes employing amplitude modulation. The examples in [7] clearly demonstrated the important consequences of choosing the resolved channel model, the importance of the pulse-shaping rolloff parameter in the frequency-selective environment, the applicability of the assumption of (12) for the frequency-selective Ricean fading case, and the advantage of considering the interfering symbols in the order of importance. While the importance of these factors was demonstrated specifically for M-PSK, their effects carry over to other higher order modulation schemes as well and will not be repeated here. In all following examples, $W = W_p$ where $W_p = 1.5/T$ is the bandwidth of the raised cosine pulse shaping with rolloff parameter 0.5. In addition, perfect AGC is assumed with the exception of the examples exploring the effects of AGC error. The same maritime high data rate (HDR) physical channel given in [7] is employed. For the Ricean fading examples, K corresponds to the K-factor of the main resolved path, and K' refers to that of the physical channel.

The first two examples demonstrate the use of the recursive solution. The flat Ricean fading case is considered in Fig. 2. The effects of the Ricean K-factor and diversity reception are clearly demonstrated for 16-QAM. As expected, the larger the KL product, the more performance improves, with most of the potential diversity performance improvement being obtained with a few multiple channels. Fig. 3 considers the frequency-selective Ricean case with the bit rate varying from 1.544 to 50 Mb/s. The K-factor of the underlying physical channel main path was fixed at $K' = 10$ dB. As the data rate is increased, the system bandwidth increases as well, and the predicted performance moves from the flat fading case to the infinite resolution frequency-selective case. Fig. 4 demonstrates the dramatic effect of a fixed AGC error in flat Rayleigh fading and frequency-selective Rayleigh fading with fixed data rate $= 1.544$ Mb/s and ϵ_{AGC} varying from 0 to 1. As can be seen, AGC tracking error results in a performance "floor" similar to that caused by intersymbol interference. It is clearly evident that a small error can dramatically change the predicted performance in certain regions. For example, even for $\epsilon_{\mathrm{AGC}} = 0.01$, performance can differ significantly from the perfect AGC case. It should be mentioned here that the $\epsilon_{\mathrm{AGC}} = 1$ curve corresponds to the poor performance predicted for the flat Rayleigh case in [2].

VI. Conclusion

This paper has extended the framework of [7] to the more general case of coherent linear modulation. This framework provides a flexible means for simultaneously evaluating the effects of key system parameters for multichannel reception in both flat and frequency-selective fading environments. General

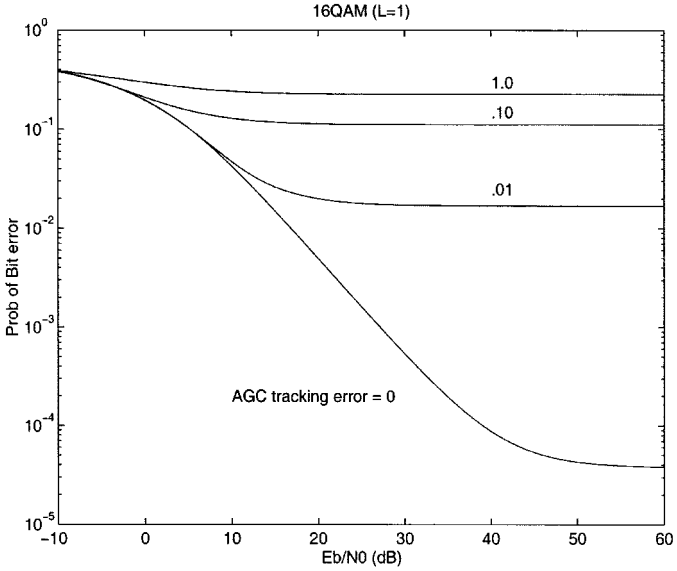

(a)

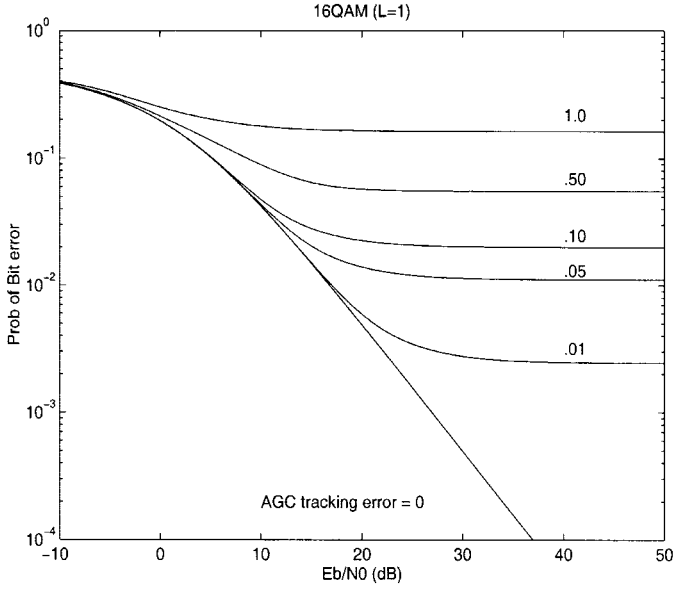

(b)

Fig. 4. Effects of AGC error. (a) Flat Rayleigh fading. (b) Frequency-selective Rayleigh fading.

results for the M-QAM modulation were provided, either in closed form or acceptably efficient numerical solutions, for special cases of practical interest. A new recursive procedure for evaluating the Ricean frequency-selective fading case was presented. The analysis framework allows exploration of the important effect of AGC tracking error. Specific bit error probabilies were obtained for 16-QAM and 64-QAM, extending the results available in current literature to the multichannel frequency-selective Ricean fading case.

REFERENCES

[1] M. Shayesteh and A. Aghamohammadi, "On the error probability of linearly modulated signals on frequency-flat Ricean, Rayleigh, and AWGN channels," *IEEE Trans. Commun.*, vol. 43, pp. 1454–1466, Feb.–Apr. 1995.

[2] P. M. Fortune, L. Hanzo, and R. Steele, "On the computation of 16-QAM and 64-QAM performance in Rayleigh-fading channels," *IEICE Trans. Commun.*, vol. E75-B, no. 6, pp. 466–475, June 1992.

[3] J. Lu, T. T. Tjhung, and C. C. Chai, "Error probability performance of L-branch diversity reception of MQAM in Rayleigh fading," *IEEE Trans. Commun.*, vol. 46, pp. 179–81, Feb. 1998.

[4] M. Alouini and A. Goldsmith, "A unified approach for calculating error rates of linearly modulated signals over generalized fading channels," *IEEE Trans. Commun.*, vol. 47, pp. 1324–34, Sept. 1999.

[5] P. Bello, "Binary error probabilities over selectively fading channels containing specular components," *IEEE Trans. Commun. Technol.*, vol. 14, pp. 400–406, Aug. 1966.

[6] F. Adachi, "BER analysis of 2PSK, 4PSK, and 16QAM with decision feedback channel estimation in frequency-selective slow Rayleigh fading," *IEEE Trans. Veh. Technol.*, vol. 48, pp. 1563–72, Sept. 1999.

[7] T. Staley, R. North, J. Luo, W. Ku, and J. Zeidler, "Performance evaluation for multichannel reception of coherent MPSK over slowly fading frequency selective fading channels," *IEEE Trans. Veh. Technol.*, vol. 50, pp. 877–894, July 2001.

[8] J. G. Proakis, *Digital Communications*, 3rd ed. New York: McGraw-Hill, 1995.

[9] I. S. Gradshteyn and I. M. Ryzhik, *Table of Integrals, Series, and Products*. New York: Academic, 1980.

[10] T. Staley, "Channel estimate-based error probability performance prediction for multichannel reception of linearly modulated coherent systems on fading channels," Ph.D. dissertation, Dept. Elect. Comput. Eng., Univ. of California, San Diego, 1997.

[11] T. Staley, R. North, R. Axford, W. Ku, and J. Zeidler, "Channel estimate-based performance prediction for coherent linear modulation on slowly fading channels," in *Proc. MILCOM'96*, vol. 2, pp. 612–617.